75rd International Astronautical Congress (IAC), Milan, Italy, 14-18 October 2022.

IAC–24–A7.3

Observing Supermassive Black Holes: Toward Optimisation of a Spaceborne VLBI Mission

Ben Hudson[1,2,*], Leonid I. Gurvits[1,3], Daniel Palumbo[4,5], Sara Issaoun[4,6], Hannah Rana[4,5]

[1] Faculty of Aerospace Engineering, Delft University of Technology, Delft, The Netherlands
[2] KISPE Limited, Farnborough, UK
[3] Joint Institute for VLBI ERIC, Dwingeloo, The Netherlands
[4] Center for Astrophysics | Harvard & Smithsonian, Cambridge, USA
[5] Black Hole Initiative, Cambridge, USA
[6] NASA Hubble Fellowship Program, Einstein Fellow, USA
[*] Corresponding Author. *Email:* benhudson@tudelft.nl

Abstract

Very long Baseline Interferometry (VLBI) provides the finest angular resolution of all astronomical observation techniques. The Earth-based Event Horizon Telescope (EHT) has demonstrated this in recent years with the landmark achievement of resolving the shadows of the supermassive black holes M87* and Sgr A*. However, these observations also showed that the science case for further sharpening the resolution of astrophysical studies is far from being exhausted. The only way to overcome fundamental limits on angular resolution of Earth-based arrays is to place part of or the entire interferometer in space. In this paper, several concepts of spaceborne VLBI systems are discussed including, TeraHertz Exploration and Zooming-in for Astrophysics (THEZA) and the Black Hole Explorer (BHEX). Spaceborne VLBI telescopes have some of the most demanding requirements of any space science mission. The VLBI system as a whole includes globally distributed elements, each with their own functional constraints, limiting when observations can be performed. This necessitates optimisation of the system parameters in order to maximise the scientific return of the mission. End-to-end mission simulations are an indispensable tool in conducting such an optimisation. Presented is an investigation into how the impact of the functional constraints of a spaceborne VLBI telescope affect the overall system performance. A preliminary analysis of how these constraints can be minimised through optimisation of the spacecraft configuration and operation is also provided. A space-based VLBI simulation tool has been developed to model such missions and its capabilities are demonstrated throughout the paper. It is imperative that the functional constraints are considered early in the design of the future space-based VLBI systems in order to generate feasible mission concepts and to identify the key technology developments required to mitigate these limitations.

keywords: VLBI, Space Observatories, Supermassive Black Holes, Spacecraft Optimisation, Astrophysics,

Acronyms

AGN	Active Galactic Nuclei
BHEX	Black Hole Explorer
DSB	Double-Side-Band
ECI	Earth Centered Inertial
EHE	Event Horizon Explorer
EHI	Event Horizon Imager
EHT	Event Horizon Telescope
ESA	European Space Agency
FOV	Field-Of-View
GEO	Geostationary Earth Orbit
GR	General Relativity
GRMHD	General Relativistic Magnetohydrodynamics
HEO	Highly Elliptic Orbit
HPOP	High Precision Orbit Propagator
ISL	Inter-Satellite Link
LEO	Low Earth Orbit
LIGO	Laser Interferometer Gravitational-wave Observatory
LISA	Laser Interferometer Space Antenna
MEO	Medium Earth Orbit
ngEHT	Next Generation EHT
SMBH	Super Massive Black Hole

SMEX	Small Explorer
SNR	Signal-Noise Ratio
SSB	Single-Side-Band
STR	Star Tracker
THEZA	TeraHertz Exploration and Zooming-in for Astrophysics
USO	Ultra-Stable Oscillator
VLBI	Very Long Baseline Interferometry
VSOP	VLBI Space Observatory Programme

1. Introduction

Space-based, Very Long Baseline Interferometry (VLBI) can achieve the finest angular resolution of current astronomy techniques. VLBI enables radio astronomers to probe the depths of Active Galactic Nuclei (AGN), as demonstrated by the ground-based Event Horizon Telescope (EHT), in 2019 and 2022. The EHT was able to resolve the shadows of the Supermassive Black Holes (SMBH) M87* and Sgr A*, with a resolution of ~20 μas at a frequency of 230 GHz [1], [2].

However, ground-based VLBI is inherently limited as the maximum baseline cannot exceed the diameter of the Earth and observational frequency is effectively constrained to below ~350 GHz, due to atmospheric absorption. The EHT has already performed observations near this limit at 345 GHz and the next generation EHT (ngEHT) will regularly use this frequency [3]. Therefore, observation at as short a wavelength as possible and on longer baselines is essential for progressing the capabilities of VLBI. This can only be achieved through the addition of a space-based VLBI system.

Two dedicated space VLBI missions have been flown as of the time of writing: RadioAstron and VSOP-HALCA, with RadioAstron ending operations in 2019 [4], [5]. Following the recent successes of the EHT, multiple concepts are being proposed for the next generation of space-based VLBI systems. In this paper, two particular concepts are focused on: TeraHertz Exploration and Zooming-in for Astrophysics (THEZA) and the Black Hole Explorer (BHEX) [6], [7].

VLBI is a particularly difficult technique to perform in space, requiring a complicated mission architecture and spacecraft design. As such, a number of functional constraints related to the system design limit when observations can be performed. This has the potential to severely reduce the science return of the mission. It is therefore essential that these constraints are identified early in the design process and are mitigated as much as possible. Presented in this paper is an investigation into the functional constraints pertaining to BHEX, THEZA and space-based VLBI in general.

Section 1.1 provides a brief overview of the VLBI technique. In section 1.2, the science objectives of the next generation space-VLBI systems are discussed. Section 2 describes the RadioAstron and VSOP-HALCA missions, focusing on the functional constraints of both systems. Other space-VLBI concepts that appear in literature are also discussed. Sections 2.2 and 2.3 provide more detailed descriptions of the BHEX and THEZA concepts. In section 4, the orbit configurations considered for BHEX and THEZA in this investigation are presented, along with rationale for their selection. In section 5, an optimisation approach for the mission design is presented to minimise the impact of the functional constraints. Section 6 includes identification of the major functional constraints impacting space-based VLBI and their specific relevance to BHEX and THEZA. Using the approach defined in section 5, preliminary optimisation of the spacecraft design and mission architecture is performed to analyse mitigation strategies for each functional constraint. Finally, in section 7, more general methods for mitigating the impact on the science return of the future space VLBI missions are presented.

1.1 VLBI

VLBI uses the principles of radio interferometry to enable signals received at different antenna to be correlated to produce a visibility function of the source. By performing an inverse Fourier transform, a brightness distribution can then be generated. The angular resolution θ of such a system is given by $\theta \approx \lambda/D$, where λ is the wavelength and D is the distance between the two antennas, projected on the plane perpendicular to the direction to the source, known as the baseline.

VLBI enables the separation between these antenna to be very large, hence providing very fine resolutions, with no physical connection between the two systems required. Observations are conducted concurrently at different facilities with a precise local frequency reference (typically an atomic clock) and time synchronisation between antenna. Data is stored on large solid state drives which are then transferred to a centralised location to undergo correlation.

A two-element interferometer provides a very sparse coverage of the source's visibility function. The measurements are obtained at spatial frequencies u and v, defining the Fourier domain of the image. The set of *(u,v)* points at which measurements of the visibility function are obtained is called the *(u,v)* coverage. Inclusion of more antenna in the interferometer array, with a variety of baseline lengths throughout the observation, results in a denser

(u,v) coverage which is required for higher-fidelity reconstructions of the source model.

1.2 Space-based VLBI Science Objectives

Space-based VLBI can enable scientific investigation that is impossible or very difficult to do from the ground. The scientific objectives of the next generation of space VLBI systems are wide ranging, with the potential to answer key questions across multiple areas of research. The primary objective of BHEX and the focus of a number of papers on THEZA is detection of a SMBH's photon ring(s) [8][9].

Photons in the vicinity of a SMBH can experience extreme deflection and complete n number of half-orbits about the black hole before escaping, causing gravitational lensing. As n increases, the observer sees exponentially demagnified images of the accretion disk, appearing as brighter, but less luminous in terms of total flux density, features [10]. As the photon ring approaches the critical curve, its structure depends increasingly on spacetime geometry and less on astrophysical phenomena [11]. However, even at low values of n, the photon ring geometry contains information on the black hole's mass and spin, and can be used to conduct strong-field tests of general relativity (GR) [10], [12]–[14]. Spin can also be constrained through other methods. Palumbo et al. shows a correlation between spin and the curl of the linear polarization pattern in the emission ring in GRMHD simulations [15]. This can be performed on sources that cannot be resolved at horizon-scale like M87* and Sgr A*, enabling BHEX to unlock a range of SMBH for which such measurements may be possible.con

On Earth baselines at 230 GHz and 345 GHZ, the EHT and ngEHT cannot yet resolve the $n = 1$ ring [2], [16]. Johnson et al. demonstrate that the interferometric signature of a black hole on very long baselines is dominated by the photon ring contribution [10]. As can be seen in Fig. 4 of Johnson et al., observation on baselines longer than ∼20 Gλ provides access to the photon ring-dominated regime [10]. Therefore, if an interferometer can observe on these long baselines with sufficient sensitivity to detect the decreasingly weak signals, the photon rings can be characterised [12], [17]. This will be possible with space-based VLBI systems and detection of the $n = 1$ ring is the primary objective of BHEX [8]. Probing $n = 2$ with future space VLBI missions would provide the most accurate tests of strong gravity to date [12], [17].

Prospective Space VLBI science does not only focus on photon ring detection. Earth-based arrays cannot yet capture the dynamic behaviour of M87* or Sgr A*, with gravitational timescales of ∼9 hours and 20 seconds, respectively [16]. Longer observations are required to study the evolution of M87* and Earth-rotation does not provide rapid enough variation in the *(u,v)* plane to capture the dynamic behaviour of Sgr A*. Space-based systems can achieve rapid filling of the *(u,v)* plane and may even enable the generation of movies of black hole evolution, from multiple image reconstructions of the source.

Space VLBI will also enable study of other AGN and their jets, providing insight into the bright, compact core feature seen in many blazars [18]. This will enable study of jet acceleration and collimation, providing a means of constraining possible energy extraction mechanisms and jet models [19]–[21].

An intriguing science case for future space-based VLBI systems is the study of sub-parsec, SMBH binary systems. Binary SMBHs are products of galaxy mergers and their inspiraling at certain stage is driven by gravitational wave (GW) emission [22]–[24] thus making them scientifically reach objects for the so-called multi-messenger astronomy. A space VLBI mission providing sufficient angular resolution and sensitivity to resolve such SMBH binaries would enable direct measurement of the system's properties. As such, multi-messenger observations of these objects, in collaboration with instruments such as LISA, LIGO and the European Virgo observatory, would provide a rich study of the origin and evolution of black hole mergers [25].

In this paper, photon ring detection and the subsequent science that can be performed with characterisation of the ring properties are considered as the primary objective of the space VLBI concepts under analysis. M87* and Sgr A* are considered as the target sources although some discussion is given to the increase in mission optimisation complexity if other sources are considered as well. Future work will investigate mission design optimisation for performing more specific AGN studies and multi-messenger observations of black hole binaries.

2. Space-Based VLBI

As stated in section 1, expansion of VLBI arrays into space is crucial to overcome the limitation on angular resolutions of Earth-based arrays. However, inherent to space VLBI design are a range of functional constraints which limit when observations can be performed. Two dedicated space VLBI missions have flown as of the time of writing: RadioAstron and VSOP-HALCA.

VSOP-HALCA utilised an 8 m antenna and operated in a Highly Elliptical Orbit (HEO), with an apogee of ∼21,400 km and an orbital period of 6.3 hours [26]. The spacecraft required a radio link with a tracking ground station to be maintained throughout observations. However, unlike RadioAstron, VSOP-HALCA did not fly a frequency standard onboard. Instead, the link with the ground station was used to transmit a high-stability signal

to feed into the onboard heterodynes. Across all precessions of its highly elliptical orbit, this resulted in a range of 0.55 and 0.85 fractions of the orbit when a ground station was available, greatly reducing the duration of potential observation periods [27].

RadioAstron utilised a 10 m, deployable antenna and also operated in a Highly Elliptical Orbit (HEO) but with an apogee near lunar in distance [28]. On the longest baselines and highest frequencies, it achieved the finest angular resolution in continuum imaging observations, 27 μas [29]. The RadioAstron User Manual provides a clear description of the observational constraints of the system and the reader is referred to that document for more detail [4]. For example, significant constraints existed in the thermal control of the spacecraft with a very limited range of Sun positions for which observations could be performed. For both VSOP-HALCA and RadioAstron, tracking from ground stations was also required to provide accurate position determination of the spacecraft which is crucial for the correlation process post observations [4], [5].

It is essential that lessons are learnt from the experience of VSOP-HALCA and RadioAstron in order to maximise the science return of future space VLBI missions [30].

2.1 Mission Concepts

Several, space-based VLBI concepts have been proposed in recent years, of varying levels of maturity. The Event Horizon Imager (EHI) concept has been discussed by several authors [31]–[33]. The EHI consists of two to three space telescopes in Medium Earth Orbit (MEO), aiming to achieve a resolution of ~5 μas with space-space baselines. The CAPELLA concept proposes two pairs of small VLBI satellites operating in polar, Low Earth Orbits (LEO) and observing at 690 GHz to provide a resolution of 7 μas [34]. Forming ground-space baselines, Fish et al. propose two spacecraft operating in a Geostationary Earth Orbit (GEO) and a HEO as an addition to the EHT, to increase resolution to 3 μas [35].

Although some of these concepts have provided commentary on the practical engineering difficulties associated with space-based VLBI, none have as of yet seriously considered the functional constraints on observations. All of the referenced concepts discuss optimising the spacecraft's orbit to meet the science objectives but do not attempt to mitigate the impact of the functional constraints. This is an essential activity, particularly when such concepts mature to the point of considering the design of the system, as the science return of the mission may be severely degraded if these issues are not tackled early in the design phase.

The two mission concepts that are considered in detail in this paper are described more fully below.

2.2 BHEX

The Black Hole Explorer (BHEX)* is a concept aiming at a NASA Small Explorer (SMEX) programme at the next call for proposals expected in 2025 [36]. The primary science goal of BHEX is to resolve the photon rings of M87* and Sgr A* to enable precise measurements of their mass and spin. This will be accomplished with a 5x increase in angular resolution compared to the EHT.

The preliminary BHEX design consists of a 3.5 m, fixed, monolithic antenna and cryogenic cooling of the receiver electronics to achieve sufficient Signal-Noise Ratio (SNR) to enable detections of the $n = 1$ photon ring. Observing across two frequency bands in collaboration with ground-based antenna, the primary receiver will be double-side-band (DSB) and operate over a frequency 240–320 GHz. A secondary receiver will be single-side-band (SSB), operating over the range 80–106 GHz [36]. Both receivers will be capable of dual-polarization measurements. BHEX's maximum observational frequency of 320 GHz is used in the subsequent generation of *(u,v)* coverage plots. BHEX will utilise a real-time, optical downlink of raw VLBI data. This system will be based on that demonstrated by NASA's TBIRD mission, achieving 100 Gbps from the reference BHEX orbit [36], [37]. A crystal ultra-stable oscillator (USO) will also be flown onboard the spacecraft to provide a stable frequency reference to achieve coherence during observations [38].

2.3 THEZA

TeraHertz Exploration and Zoming-in for Astrophysics (THEZA) is a concept that was prepared in response to the European Space Agency's (ESA) call for its next science program Voyage 2050 [6], [39]. By observing at millimeter and sub-millimeter wavelengths, THEZA aims to achieve at least an order of magnitude improvement on the EHT's angular resolution. The THEZA concept consists of at least two spaceborne antennas, forming space-space baselines.

Although THEZA has not undergone a detailed mission design exercise, key elements of the system have been discussed [6], [9], [39]. Two methodologies are presented for the handling of the large volumes of VLBI data for THEZA. As with BHEX, the use of optical communications systems onboard is proposed to downlink the data to the ground. An alternative architecture consisting of in-orbit correlation by transferring the data from one spacecraft to the other via optical Inter-Satellite Link (ISL) is

*https://www.blackholeexplorer.org/

also discussed [39]. The latter being a more forward-looking approach that would require significant computing capability onboard. As such, in this paper, downlink of science data to the ground via optical terminal to a set of dedicated, optically-capable ground stations is considered in the evaluation of the impact of the functional constraints.

BHEX will be considered as the primary mission concept under analysis for the rest of the paper. If accepted as a SMEX mission, analysis of the functional constraints impacting BHEX is practically useful as the mission will soon enter a design phase in which investigations such as this will be crucial. BHEX represents the current capabilities of potential space-based VLBI systems. THEZA offers a view of the future of space VLBI, with multiple space telescopes and observation at very high frequencies providing an order of magnitude improvement in angular resolution. Therefore, some discussion of the impact of the investigation performed in this paper on THEZA is also included.

3. Mission Simulation: `spacevlbi`

In order to model space-based VLBI missions, the Python package `spacevlbi` has been developed. `spacevlbi` is capable of high fidelity modelling of a space telescope's orbit and attitude state. Ground VLBI antennas can also be modelled, enabling ground-space VLBI simulations. By defining a ground array, a space telescope orbit and a target source, `spacevlbi` provides the *(u,v)* coverage achieved over the simulation time period. Multiple space telescopes can also be modelled simultaneously, enabling simulation of missions such as THEZA.

The attitude of the space telescope is modelled throughout the simulation by defining a body-fixed axis to point towards a target source. By modelling the attitude of the spacecraft, the directions in which key onboard instruments and subsystems such as the antenna, solar panels, optical terminals, star trackers and radiator surfaces are pointed can be determined.

Unlike other VLBI simulation packages, the functional constraints of a space-based mission can be modelled in `spacevlbi`. This will also make the tool of use during conceptual and detailed design phases of future space-based VLBI systems, allowing the practical considerations of spacecraft design to be combined with more detailed science simulations such as those that can be performed in packages like the `eht-imaging` library [†] [40]. The functional constraints that can be modelled in `spacevlbi` cover a wide range of traditional spacecraft subsystems and the reader is referred to the documentation of the publicly available tool for more information on its capabilities [‡].

`spacevlbi` is used to perform all of the analysis presented in this paper. *(u,v)* coverage figures are based purely on the geometry of the interferometer and the target source and do not take into account the effects of weather conditions at ground antenna sites or the SNR of detections. For the purpose of demonstrating the impact of functional constraints, characteristics of real VLBI observations such as the integration time, length of each scan and the cadence that scans are performed at have also not been considered in the analysis. The optimisation approach and analysis of missions such as BHEX presented here is agnostic of the values of these parameters.

4. Orbit Configuration

Orbit selection for science missions is typically a trade-off between what is optimal to meet the scientific objectives and feasibility from an engineering perspective. Preliminary orbits are being considered for BHEX based on the scientific objectives of the mission and some consideration of the engineering implementation. However, analysis of the functional constraints will be required regardless of the final orbit selection and it is the methodology presented in this paper that is the focus.

A favoured candidate for BHEX is a circular, polar MEO with an orbital radius of 26564 km [36]. The 12 sidereal hour period of this orbit generates a repeating ground-track which makes determination of optical ground terminal locations to provide continuous coverage of the spacecraft simpler. The right ascension of the ascending node has been selected to set the orbit plane almost perpendicular to the direction of M87* but slightly rotated to increase the coverage of Sgr A* in the *u*-plane. The inclination also provides a compromise between the declinations of M87* and Sgr A*, 12.4 and -29.0°, respectively.

This orbit provides the required space-ground baseline coverage of both sources to theoretically detect the first order photon ring. The full baseline range offered by BHEX in collaboration with the specified ground-based array is ∼18-33 Gλ (M87*) and ∼2-34 Gλ (Sgr A*), at 320 GHz [10]. The unconstrained *(u,v)* coverage achieved by BHEX in collaboration with an extensive ground array (see Fig. 1 for definition of the ground array) is shown in Fig. 2. A minimum observing elevation of 15° is assumed at each ground station.

In our previous work [9] is presented a number of orbit configurations for a spaceborne, two-element THEZA

[†] `https://github.com/achael/eht-imaging`

[‡] `https://github.com/bhudson2/spacevlbi`

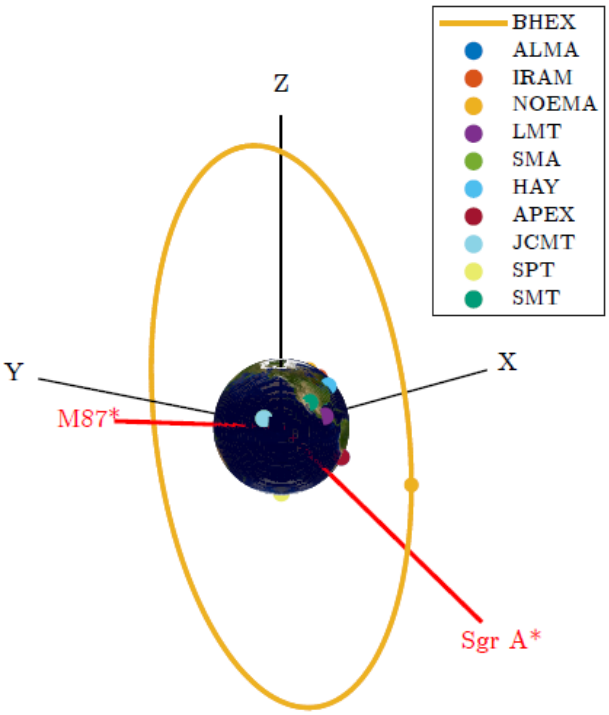

Fig. 1: Preliminary BHEX orbit for the detection of the $n = 1$ photon ring in M87* and Sgr A*.

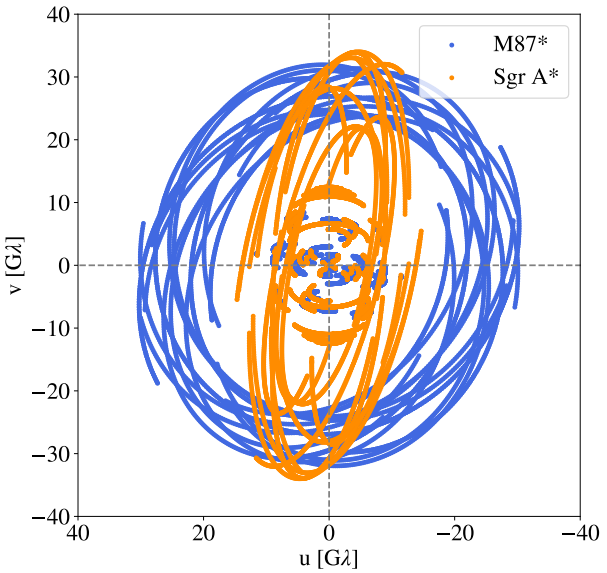

Fig. 2: An "ideal" *(u,v)* coverage for M87* and Sgr A* achieved by BHEX in the reference orbit. Observation conducted with ground array depicted in Fig. 1, at a frequency of 320 GHz, over 24 hours.

system, utilising 15 m antennas and optimised for the detection of photon rings [9]. The configurations have been designed to achieve a wide variation in baseline length of 20-200 Gλ, regardless of the position of the source on the sky.

Fig. 3 depicts the circular, coplanar MEO configuration of THEZA from [9]. The right ascension of the ascending node of the orbits has been set to the average of M87* and Sgr A*, maximising *(u,v)* coverage for both sources (depicted in Fig. 4). The starting true anomaly of either spacecraft can be set to any value and the required baseline variation will still be achieved within 7 days.

The reference BHEX orbit and the THEZA orbit depicted in Fig. 3 are used as the example configurations of the two interferometers in the subsequent functional constraint analyses.

5. Mission Optimisation

Various methodologies have been proposed for spacecraft configuration design optimisation [41], [42]. These methods optimise only specific component positions: radiators and star tracker, respectively. Furthermore, most optimisation processes utilise a genetic algorithm which mimics natural evolutionary processes on an initial population of potential solutions to converge on an optimal result. Genetic algorithms are an effective way to optimise multi-parameter, multi-objective problems with a large search space, but they can miss optimal solutions by finding local rather than global minima.

Presented in this section is a configuration optimisation method, using MaVS, that enables the optimal position of spacecraft components with external Fields of View (FOV) to be determined. This method is useful for positioning items such as star trackers, radiator surfaces, communication systems and solar panels, or any other units whose performance is dependent on a specific relationship with the Sun, Earth or Moon. Unlike other approaches, this method can be used to optimise the position of a variety of component types. It also evaluates the entire search space, providing the user with all possible, optimal configurations, given the constraints from the spacecraft model.

This method has been developed in order to find an optimal spacecraft configuration to minimise the impact of the functional constraints on observations. Unlike the cited methodologies, this approach takes a systems view of the problem, considering various subsystems concurrently rather than specific units in isolation. The method is based upon mission simulation in MaVS (presented in section **??**), which utilises the DE440 JPL Planetary Ephemeris files to provide Sun and Moon positions [43]. This enables highly accurate and time-dependent analy-

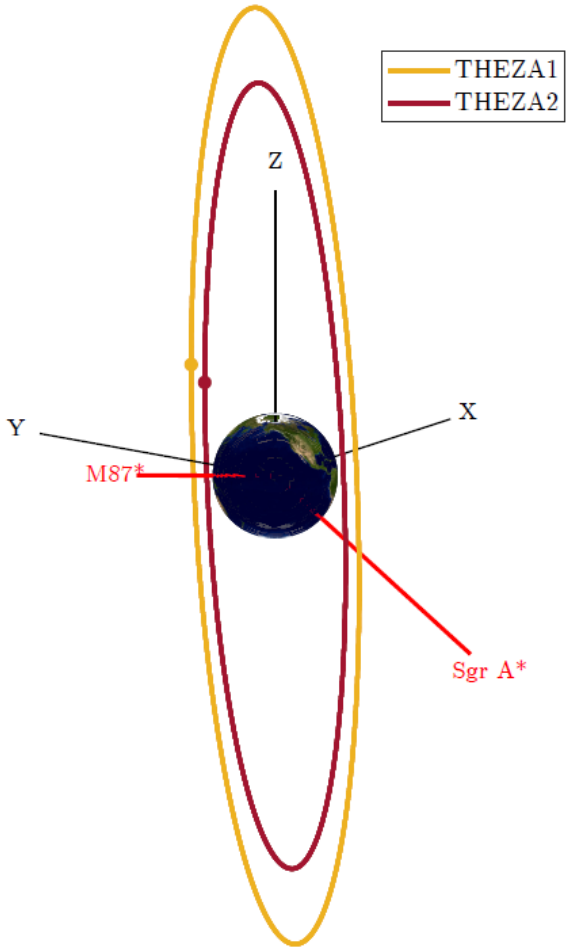

Fig. 3: Circular, coplanar, polar orbit configuration of THEZA, for the detection of the $n = 1$ and $n = 2$ at 690 GHz [9].

ses of the impact of Sun, Earth and Moon position on the spacecraft operation.

Use of the *attitude sphere* is the core of the optimisation method. An attitude sphere depicts the spacecraft body-fixed axis, the pointing of various components and the positions of the Sun, Earth and Moon, over a given period of time. Fig. 5 depicts the attitude sphere of BHEX, operating in the reference orbit. It shows the Sun, Earth and Moon positions when observing M87* across a 24 hour period. The optimisation method is then performed as shown in Fig. 6.

The optimisation process is run using a single or multiple completed MaVS simulation(s). This enables the optimisation to be conducted for varying simulation properties, for example, observing different sources. The simulation results are used to evaluate the *fitness* of each potential component position onboard the spacecraft. All possible positions for components are evaluated with the generation of unit vectors, in which the component may point, that cover the entire attitude sphere. This search space can also be reduced based on a number of fixed constraints. This allows users to focus on particular areas of the spacecraft, if it is already known that some positions are unsuitable (E.g. for BHEX, with the antenna pointed in Z-direction, it is unlikely star trackers can point in the same direction).

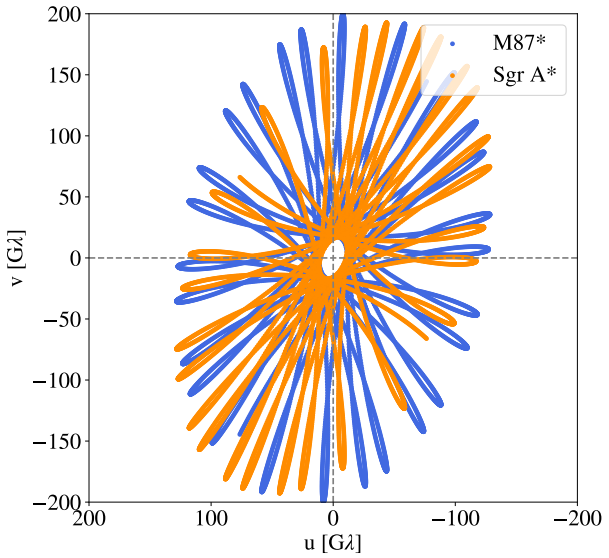

Fig. 4: An "ideal" *(u,v)* coverage for M87* and Sgr A* achieved by THEZA in the orbit depicted in Fig. 3. Observation conducted at 690 GHz across 7 days.

The fitness of a position is dependent on the specific component being optimised and a bespoke function must be developed for each. This is because the evaluation criteria may vary between components. Some examples applicable to VLBI include:

1. Star trackers/radiators: fitness is number of time steps for which neither the Sun, Earth or Moon falls within the component FOV
2. Real-time, optical communications system: fitness is the number of time steps for which the Earth falls within the component FOV
3. Solar panels: fitness is the number of time steps for which the solar incidence angle is less than a defined value for maximising power generation

Once this process is complete, lists of potential configurations of the components under investigation are provided, along with their fitness. This process has been followed

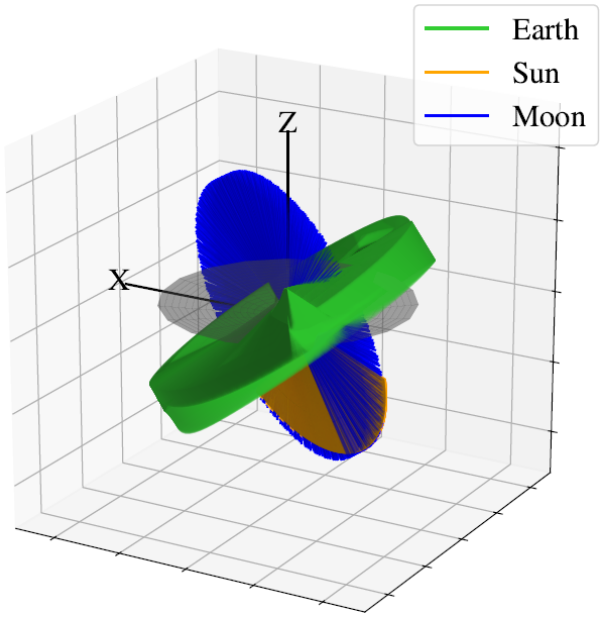

Fig. 5: Attitude sphere showing BHEX antenna configuration and Sun, Earth and Moon positions throughout Jan–Apr observation season of M87*.

to identify optimal configurations for the BHEX example mission in the subsequent sections, in order to minimise the impact of functional constraints on observations.

6. Functional Constraints

Space mission development is an iterative process whereby a design slowly converges to a point where it meets all of the mission requirements. Trade-offs are an inherent part of spacecraft design and identification of the key trade spaces and resolution of these conflicts is a core part of the development process (i.e. the needs of one subsystem are often not compatible with those of another).

Although the design of a VLBI mission will follow this same process, it is unique amongst science applications in the complexity of its operation. Not only does it require a highly performant spacecraft, the mission architecture consists of multiple, complex relationships with systems on the ground (E.g. ground radio antenna and tracking ground stations). As such, space-based VLBI poses a unique design study, one that warrants a bespoke methodology in the optimisation of the system's characteristics.

In this section, an investigation into the functional constraints that impact space VLBI missions is performed, along with an assessment of how these will limit observations. Specifically, the BHEX concept is used as a case study. However, discussion of how the constraints are relevant for other concepts such as THEZA is also considered. The subsequent investigation is organised by traditional spacecraft subsystem.

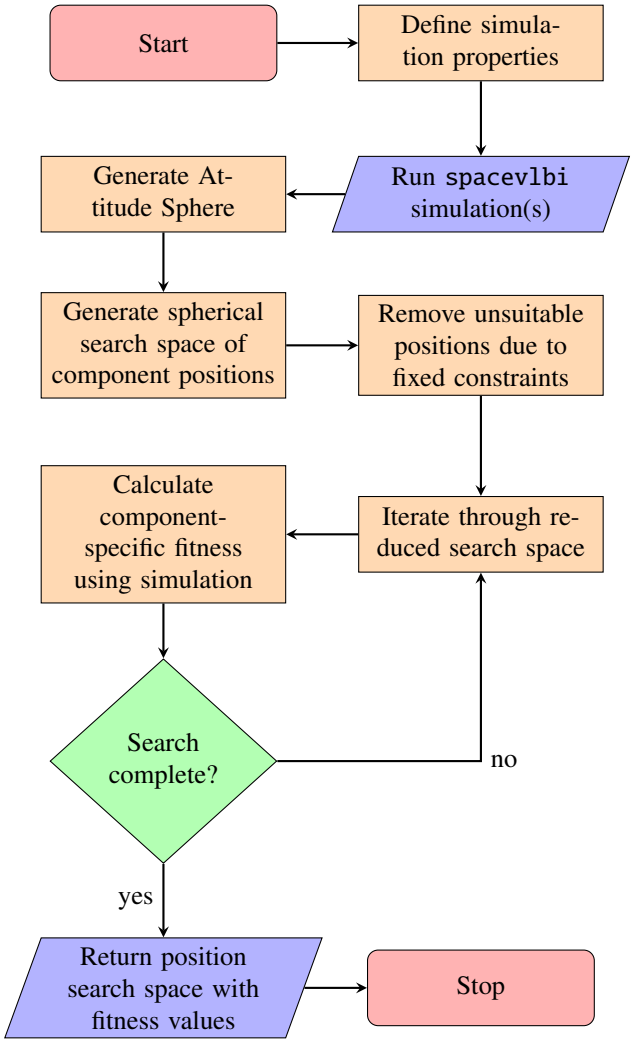

Fig. 6: `spacevlbi` spacecraft configuration optimisation process to minimise the impact of functional constraints on observations. Used for the positioning of components with Earth/Sun/Moon-dependent performance.

6.1 Science Data Communications and Handling

Data handling of a space VLBI mission is a particularly challenging aspect of the design. VLBI requires operation at very wide bandwidths to increase sensitivity and therefore, data is recorded at extremely high rates. For a 24 hour observation, a single interferometer element might generate terabytes of data. Since 2018, the EHT has been operating at 64 Gbps [1]. A trade-off exists between the implementation of mass data storage onboard

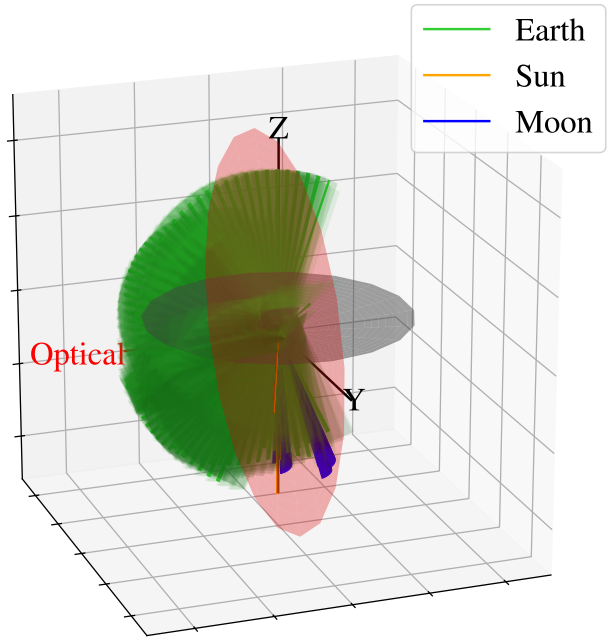

Fig. 7: Attitude sphere showing optimal BHEX optical terminal configuration and Sun, Earth and Moon positions during observation of M87* and Sgr A* (1st Jan and 1st June, respectively.).

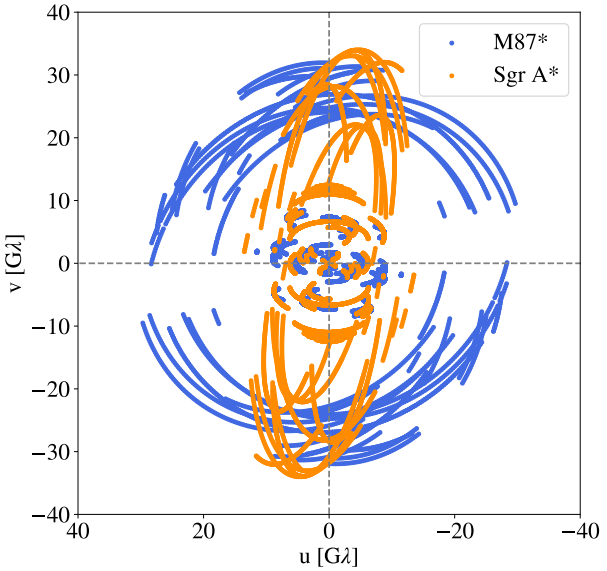

Fig. 8: 24 hour *(u,v)* coverage of M87* and Sgr A* by BHEX on 1st Jan and 1st June, respectively. Observations limited to when an optical downlink with the ground is achievable. Terminal gimbal capability limited to ±70°. 45.5% and 36.8% loss in coverage of M87* and Sgr A*, respectively.

and the real-time downlink of data to the ground. Gurvits et al. provide a thorough description of this trade-off and the current state of the technology required for both options [39].

The current concept of operations for BHEX involves the use of a real-time downlink of data, using an optical communications terminal. This system is based on that demonstrated by the TBIRD mission, which has demonstrated downlink rates of up to 200 Gbps [37], [44]. The optical communications system will be gimballed, allowing it to point independently of the spacecraft's attitude. The limit of the gimbal capability is still under consideration, and the effect of varying this is presented in the subsequent analysis.

During observations, BHEX would ideally remain in an inertially-fixed attitude in order to point the antenna at the target source and minimise variation in the polarisation of the received signals. Therefore, the Earth-facing side of the spacecraft would vary throughout observations, as the spacecraft moves around its orbit. Under these restrictions, the optimal position for the unit is in the opposite direction to the antenna, with the nominal pointing direction along the negative Z-axis. This was calculated with the process described in section 5. With the gimbal capability, the terminal can then point in any direction in the negative Z-plane. Observation of either source can only take place if an optical link can be maintained with an array of ground stations, distributed across the globe. A minimum elevation at each ground station of 15° is assumed. For this analysis, a set of four ground optical sites distributed across the globe are considered: Perth Australia, Haleakala Hawaii, Achaea Greece, La Silla Chile. These sites have been preliminarily selected for BHEX as they provide constant coverage of the orbit.

This configuration results in a loss of 44% and 49% of *(u,v)* coverage when observing M87* and Sgr A*, respectively. This unacceptable constraint on observations could be mitigated through a number of methods:

- Inclusion of mass data storage for onboard buffering of VLBI data during periods of the orbit when a link with the ground cannot be achieved
- Multiple optical communication terminals located around the spacecraft bus
- Position of the optical terminal and rotation of the spacecraft about the antenna direction (Z-axis), at intermittent points during observations, to keep the Earth within the FOV of the gimballed terminal

The last solution is the most feasible, given the programmatic constraints of the BHEX programme. Fig. 7 depicts an optical terminal configuration that provides a constant

real-time downlink with ground stations, when observing M87* and Sgr A*. The terminal is mounted in the spacecraft +X axis and every half orbit period, the spacecraft is rotated 180° about the +Z axis to keep the Earth within the optical terminal FOV. By performing this rotation, the variation in polarisation of the received signals is negated. This strategy also provides a deep-space facing side of the spacecraft that would be highly beneficial for the mounting of star trackers and thermal components. This is discussed in more detail in the following sections.

The proposed configuration does require that the optical terminal is mounted such that the antenna surface is not within its FOV. The terminal would need to be mounted such that it protrudes past the antenna surface. A more detailed mechanical analysis is required to assess the feasibility of this. Furthermore, if the gimbal capability is any less than the optimal ±90°, the positions in the orbit at which a downlink with the ground can be achieved begin to reduce. with a gimbal capability of ±70°, the *(u,v)* coverage of M87* and Sgr A* is reduced to that depicted in Fig. 8.

Even if the data downlink constraint is mitigated through one of the methods discussed previously, there is still the challenge of frequency standard provision and tracking for fine orbit determination. If a local frequency standard is not included onboard, a link with the ground is required throughout observations to provide a stable reference signal, as was the case with VSOP-HALCA [5]. This constraint is removed if an atomic clock is flown onboard, as demonstrated by RadioAstron with a Hydrogen Maser and this is also the intention for BHEX [4], [38]

Tracking of the spacecraft is required to accurately reconstruct the spacecraft's orbit so that it's position is known throughout observations for the correlation process. A network of ground tracking stations is required to achieve this, above altitudes where GNSS can be used. For BHEX, the optical ground station network could be utilised to perform ranging from the ground, enabling accurate reconstruction of the orbit. However, for future space VLBI missions perhaps not utilising a real-time downlink, fringe finding during correlation may not be possible for parts of the spacecraft's orbit with insufficient position accuracy. Gurvits et al. provide a more complete description of these challenges [39].

6.2 Thermal Constraints

For space-based VLBI it is essential that the Sun does not illuminate the science antenna opening as this can result in heating of the critical components in the radio signal chain, parts of which must be cooled to very low temperatures in order to reduce thermal noise. The Sun also produces radio signals and therefore is a source of noise on the science measurements.

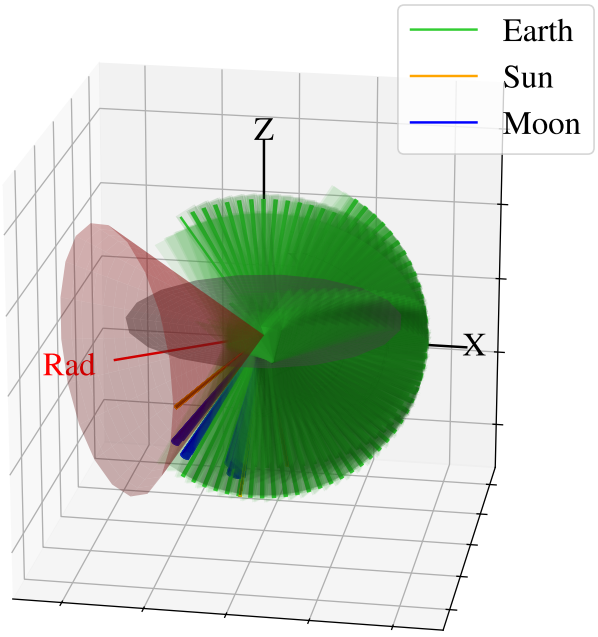

Fig. 9: Attitude sphere showing optimal BHEX radiator configuration if a baffle with a ±40° FOV is implemented to shade the surface. Sun, Earth and Moon directions during observation of M87* and Sgr A* (1st Jan and 1st June, respectively.) are also shown.

As such, it is required that the Sun does not fall within the FOV of the antenna when observations are being performed. For example, RadioAstron could not perform an observation if the Sun fell within 90° of the antenna boresight [4]. For the same reason, there are typically limitations on the Earth and sometimes Moon position during observations, due to its thermal emission. RadioAstron could not observe if the Earth limb or Moon was within 5° of the antenna boresight [4].

Various strategies can be used to reduce this Sun exclusion requirement such as the use of Sun shields and shading of the antenna surface. However, these approaches can add significant mass and complexity to a mission, particularly in the case of a Sun shield which will often require a deployable mechanism, such as that used for the James Webb Space Telescope (JWST) [45]. For analysing the impact of the Sun exclusion angle on BHEX and THEZA observation operations, a 90° limitation between the solar direction and antenna pointing is considered as this is not dependent on additional Sun shields or antenna shading systems. 5° Earth limb and Moon exclusion angles are used as preliminary values for BHEX analysis.

As would be expected, for half of the year the angle between the antenna boresight and the Sun is greater than

Table 1: Loss of *(u,v)* coverage during observation seasons of M87* and Sgr A* (i.e. the time that the radiator is not deep-space pointing). Variation shown for different radiator baffle angles, defined as a cone around the radiator surface normal vector. Use of a different baffle angle results in the optimal location for the radiator varying.

Baffle Angle [±°]	Radiator Normal	M87*	Sgr A*
40	[-0.809, -0.588, 0]	0.3%	6.7%
50	[-0.809, -0.588, 0]	38.6%	10.3%
60	[0, 1, 0]	13.6%	65.5%
70	[0.309, 0.951, 0]	17.9%	74.0%
80	[0, 1, 0]	23.9%	90.96%
90	[-0.809, 0.588, 0]	67.6%	89.8%

90° for either source (see Fig. 12 in section 6.4 for illustration of this). Therefore, observation of any source is restricted to a 6 month period each year, without consideration of any other limitations. For the BHEX mission, this observing *season* is further restricted to times of the year which are most favourable for observations from the ground sites' perspective. BHEX is planning to observe M87* and Sgr A* for 3 month periods between January-April and June-September, respectively [36]. These are therefore the times of year for which other elements of the spacecraft design should be optimised for, to minimise the impact of the functional constraints on observations.

As is evident from the attitude sphere depicted in Fig. 7, for part of the orbit, the Earth falls within 45° of the antenna boresight when observing Sgr A*. This occurs when the source is blocked by the Earth and therefore observations cannot take place anyway. However, during this period, for around 3.75 hours every orbit the antenna will be heated up by the Earth's thermal flux which will result in variation of the surface geometry. A full thermal analysis will be required to assess whether any cooling period is required before observations can commence after a period of time spent behind the Earth.

To increase the sensitivity of the instrument, the receiver electronics on BHEX will be kept at ~4.5 K during observations via cryogenic cooling [46]. The cyrocooler will require two radiator surfaces for operation: a deep-space pointing, passive heat rejection stage and a warm end heat rejection surface. The latter could occasionally be Sun pointing, the limits of which will depend on a more detailed thermal analysis of the mission. The heat rejection stage must be deep-space pointing throughout observations. The strategy proposed in section 6.1, whereby the spacecraft is rotated every half orbit period to keep one side approximately Earth-facing, is highly beneficial for the thermal control of the system. Assuming that the optical terminal is pointed along the +X axis, positioning of the radiator surface on one of the perpendicular body-axis could provide the required deep-space pointing.

The ideal pointing for a radiator surface would be in the antenna direction as this will always be pointed towards deep-space during observations. However, with a 3-4 antenna diameter, this would very likely require a deployable structure to provide an unobstructed deep-space view for the radiator. It is highly preferable to avoid such mechanisms if possible, as they add mass, complexity and cost to the mission. With this constraint in mind, there is no available position for a radiator surface for which the Earth or Sun doesn't fall within 90° of its normal vector, when observing M87* or Sgr A*. To minimise the impact of blinding of the radiator surface on observations, some baffling of the radiator will be required to shield it from the Earth and Sun.

Fig. 9 depicts the optimal position for a radiator surface with a baffle limiting its FOV to ±40°, calculated using the process in section 5. The attitude sphere shows the Sun, Earth and Moon positions for only a single day of observations for clarity. In reality, the optimal radiator positioning has been determined considering the wider range of Sun and Moon positions across the full observation season of each source. As can be seen in Fig. 5, the Sun and Moon positions form large arcs across the attitude sphere during the observation season, further limiting the acceptable positions for a radiator.

The radiator configuration shown in Fig. 9 would be deep-space pointed for the majority of the M87* and Sgr A* observation seasons. Observation of M87* is unaffected but for ~6 days of the Sgr A* season, the radiator would be blinded by the Sun. However, increasing the baffle angle results in the radiator being pointed towards the Earth or Sun for longer periods of time, during which observations cannot be performed. The optimal location of the radiator surface also varies if less shading is implemented. Table 1 shows the percentage loss in *(u,v)* coverage of M87* and Sgr A* during their observation seasons due to the radiator not being deep-space pointed. How this varies with baffle angle is also provided along with the optimal radiator position for a given baffle angle. ±90° is a radiator surface with no baffle / shading. Some of the proposed radiator positions are only suitable if the antenna surface obscuring its FOV is not impactful or, if it is, the radiator can be mounted in such a way as to remove the obstruction.

Positioning of the radiator surfaces on a space-based VLBI mission is a challenging issue and one that cannot simply be solved by adding more radiators without incurring significant mass and cost increases. Baffling of the radiator requiring deep-space pointing is likely to be essential for minimising the impact on observations to an

acceptable level. Further thermal analysis is required to consider the positioning of the warm end rejection surface to determine what level of Sun exposure is acceptable.

6.3 Attitude and Orbit Control

The Attitude and Orbit Control System (AOCS) of a space-based VLBI mission places a number of functional constraints on when observations can be performed. Space VLBI requires highly accurate and stable attitude control in order to point a very narrow antenna beam towards the target source. As such, the attitude control accuracy needs to be on the order of arcseconds (see RadioAstron attitude control: ±10" [4]). This requires utilisation of a stellar-gyro system using star trackers and gyroscopes (the most accurate attitude determination method available), and reaction wheels for attitude control. This is a standard attitude control method for space astronomy missions with similar pointing requirements (see James Webb Space Telescope, Hubble, etc. [45]).

A star tracker is a digital camera that maps the stars observed within its FOV to an internal star catalogue. By identifying the stars in the image, a star tracker can estimate the spacecraft attitude by determining the orientation of the star field with respect to the Earth Centered Inertial (ECI) frame [47]. Star trackers exhibit the highest error in orientation estimation about their boresight (i.e. pointing direction). In order to achieve arcsecond-level estimation at a system level, this typically requires two star trackers, mounted at at least 45° to each other [4], [47]. Star trackers can be blinded when the Sun, Earth and sometimes Moon, fall within their FOV. At such times, they cannot provide an attitude estimation and therefore for space-VLBI, observation cannot take place.

Consider the BHEX mission, utilising a minimum of two star trackers to provide the required attitude determination. The star trackers must be positioned to minimise the times throughout the year that they are blinded by Sun, Earth or Moon. The optimisation problem is complicated by the fact that the star tracker blinded times should be minimised for both M87* and Sgr A*. If the operational approach described in section 6.1 is utilised, the spacecraft is rotated by 180° each half orbit period to keep the Earth within the optical terminal FOV. The real-time downlink requirement is the most constraining element of BHEX's design so it is likely that minimising its impact will drive the concept of operations. Using this method, the Earth is kept within one half of the spacecraft's attitude sphere, as shown in Fig. 10. This is in fact beneficial for the placement of components that require deep-space pointing as one side of the spacecraft would always be kept away from the Earth.

However, as the spacecraft is rotated 180° about the Z-axis each half orbit, the Sun positions on the attitude sphere are effectively doubled. This can be seen in Fig. 10 as there are four distinct Sun position arcs for observing M87* and Sgr A*, rather than the expected two. This complicates the star tracker positioning. With the antenna pointed in the +Z axis, unless the star trackers are mounted such that they are not obscured by the antenna surface, it is reasonable to assume that they cannot be mounted with the boresight pointing in a +Z direction. This further constrains the available position of the star trackers, effectively to the −Z quadrant of the attitude sphere. The attitude sphere in Fig. 10 depicts the optimal locations for two star trackers, under the array of conditions stated above. These positions offer minimal blinding during the observation season of each of the primary sources, whilst meeting the criteria of having a 45-90° separation between their boresights. Sun blinding is avoided completely as this would result in entire days during which observations would not be possible. The unit vectors of the star trackers in the body-fixed frame are: [-0.476, -0.655, -0.589] and [0, 0.707, -0.707]. Fig. 11 shows the *(u,v)* coverage of M87* and Sgr A*, when star tracker blinding constrains observation times.

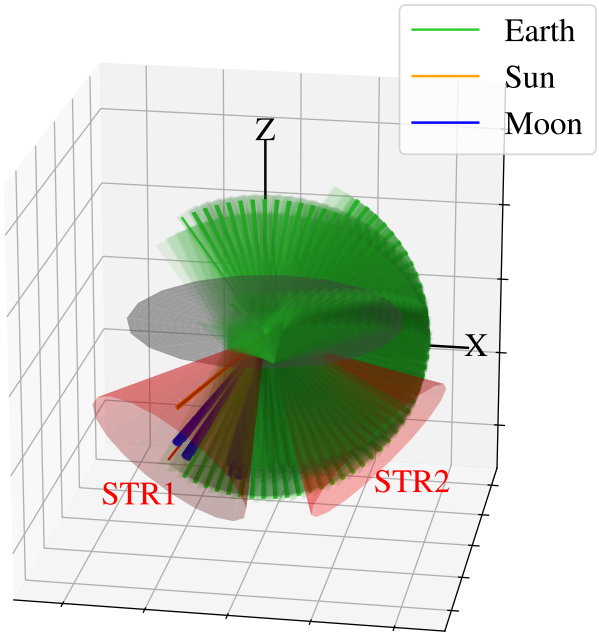

Fig. 10: Attitude sphere showing optimal BHEX star tracker (STR) configuration and Sun, Earth and Moon positions during observation of M87* and Sgr A* (1st Jan and 1st June, respectively).

Mitigation of the star tracker functional constraint could be achieved by flying a third star tracker in a hot redundant state. This unit could then be positioned to pro-

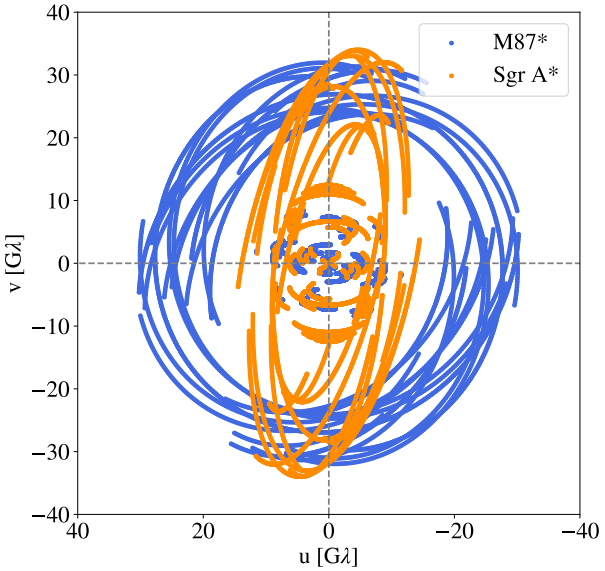

Fig. 11: 24 hour *(u,v)* coverage of M87* and Sgr A* by BHEX on 1st Jan and 1st June, respectively. Observations limited to times when neither star tracker is blinded. 15.4% loss of coverage for both M87* and Sgr A*.

vide coverage for when either of the other star trackers are blinded. Such decisions are why analysis of the functional constraint impact is crucial early in the spacecraft design process. However, this configuration optimisation has considered only M87* and Sgr A*. Observation of other sources adds another set of Earth, Sun and Moon positions to the attitude sphere which would make the positioning of the star trackers even more complex (see section 7 for a more detailed discussion on this).

Other functional constraints related to the AOCS exist but are not discussed in detail in this section. These constraints will place additional limitations on when observations can be performed, although they are unlikely to be as stringent as the star tracker placement.

- Breaks in observations during reaction wheel desaturation
- Performance of orbit station-keeping or transfers, during which a fixed antenna cannot be pointed at the target source

In relation to concepts such as THEZA, the impact of the star tracker constraint can be massively reduced if the mission is operated far from the Earth. As shown clearly in Fig. 10, the Earth covers the greatest area of the attitude sphere for a mission such as BHEX.

6.4 Power

The payload of a space-based VLBI mission, consisting of: multiple receivers, cryogenic cooling syste, ultra-stable oscillator and an optical communications terminal, will have a considerable power requirement. The optical communications system on TBIRD alone (that which the BHEX terminal will be based on), has a power requirement in excess of 100 W [44]. Whilst the power system design will be very dependent on the specific mission, a high-level investigation into the geometry of the Sun and the likely solar panel configuration of such a spacecraft can be performed to investigate the functional constraint the power requirement may place on the mission.

As described in section 6.2, observation of a given source requires that the angle between the antenna pointing and the Sun direction is greater than 90° (perhaps slightly less if some shading of the antenna is included). Therefore, the logical position for the solar panels is in the opposite direction to the antenna as this is approximately where the Sun will be located during observations. As such, consider a fixed solar panel design pointing in the negative Z-axis. The power generated by a solar panel is dependent on the characteristics of the solar cells utilised, the panel area and incidence angle of the Sun. The power generated varies in proportion to the cosine of the incidence angle of the solar radiation, measured from the panel normal. Fig. 12 shows the variation in this angle throughout the year, when observing either of the main sources.

Solar panels suffer from performance degradation throughout their lifetime due to damage from radiation and micrometeorite impacts. Therefore, they are typically sized such that they provide sufficient power at the end of the spacecraft's lifetime, considering these degradation factors. In order to provide the required power to a VLBI payload when the solar incidence angle is not 0° with respect to the panel normal, the solar panel area will need to increase by a factor equal to the reciprocal of the cosine of the incidence angle.

For BHEX, observations of M87* and Sgr A* are planned to take place during specific seasons, during which the Sun avoidance angle requirement is met. A similar strategy is likely to apply to any space-based VLBI mission observing these sources. As can be seen in Fig. 12, for ~30% of the M87* observation season, the solar incidence angle on a -Z panel is greater than 60°. For this period of time, the power generation of this panel would be 50% of that when the solar incidence angle is 0° and thus, the panel would need to be twice the area for observations to take place.

As such, there is a clear trade-off between the configuration of the solar panels and the times of year at which

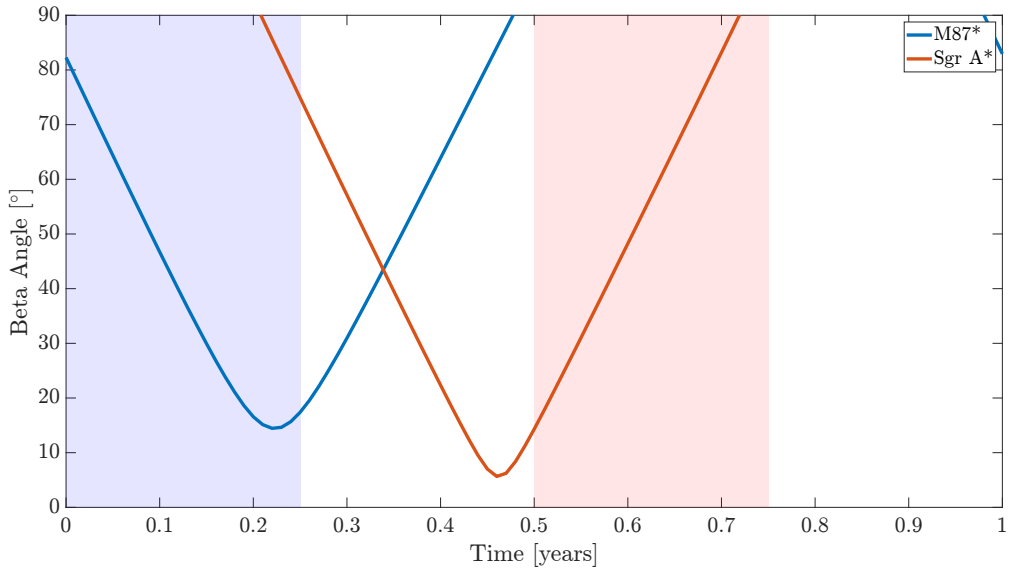

Fig. 12: Angle from solar panel normal pointed in the negative Z-axis to the incident solar radiation (beta angle). Variation shown for observation of M87* and Sgr A*. Observation seasons for both sources highlighted.

sufficient power is provided to the VLBI payload in order to conduct an observation. Several mitigation strategies exist for this constraint:

- Additional, fixed solar panels, pointing in different directions
- Use of steerable solar panel(s)
- Shift the observing season such that the angle on a -Z facing panel is closer to zero for a longer period
- Operational mitigation: periodic interruptions in observations to point the solar panels towards the Sun and charge up batteries

Each of these strategies require the resolution of a trade-off with other elements of the system and its operation. The addition of solar panels or the use of steerable systems adds significant mass to the system. Steerable panels also introduce considerable complexity as the mechanism is a mission-critical component. Furthermore, they may be outside of the financial scope of a NASA SMEX mission for BHEX. The observation season is also driven by factors beyond just this power constraint (see section 6.2).

The power constraint will need to be overcome for any space-based VLBI mission. Although this is indeed a design challenge that applies to all space observatories, it will likely still limit when observations can be performed and subsequently, the science return of the mission.

7. Mitigating Impact on Science Return

So far, each of the presented constraints have been analysed in isolation. The *(u,v)* coverage figures showing the impact on observations have not included the effect of the other constraints. In reality, the functional constraints may stack up, resulting in a boolean product of the time intervals at which observations can be performed. It is the combination of the constraints that will drive the availability of the system and thus, the science return of the mission.

The future space-based VLBI missions must of course be designed to minimise the impact of these (and other) functional constraints. However, as has been shown in the previous sections, the complexity of performing VLBI in space means that the number of functional constraints makes it highly unlikely that they will all be completely mitigated. As has been discussed, strategies exist to reduce, and in some cases, negate the impact of these constraints. For example, inclusion of additional star trackers, positioned in such a way as to have at least two that are never blinded. Various methods have been proposed for removing the real-time optical downlink constraint; mass data storage being the obvious solution. The difficulty is in implementing these strategies within the mass, power and and financial envelope of the mission. A typical mass limit of a NASA SMEX spacecraft is ~200-300 kg [48]. This, together with other programmatic constraints of a SMEX mission are likely to be the limiting factors in overcoming the functional constraints of the mission.

Furthermore, the constraint analysis in this investigation has focused on the two largest sources as seen from the Earth: M87* and Sgr A*. As described in section 1.2, the science applications of VLBI require wider observa-

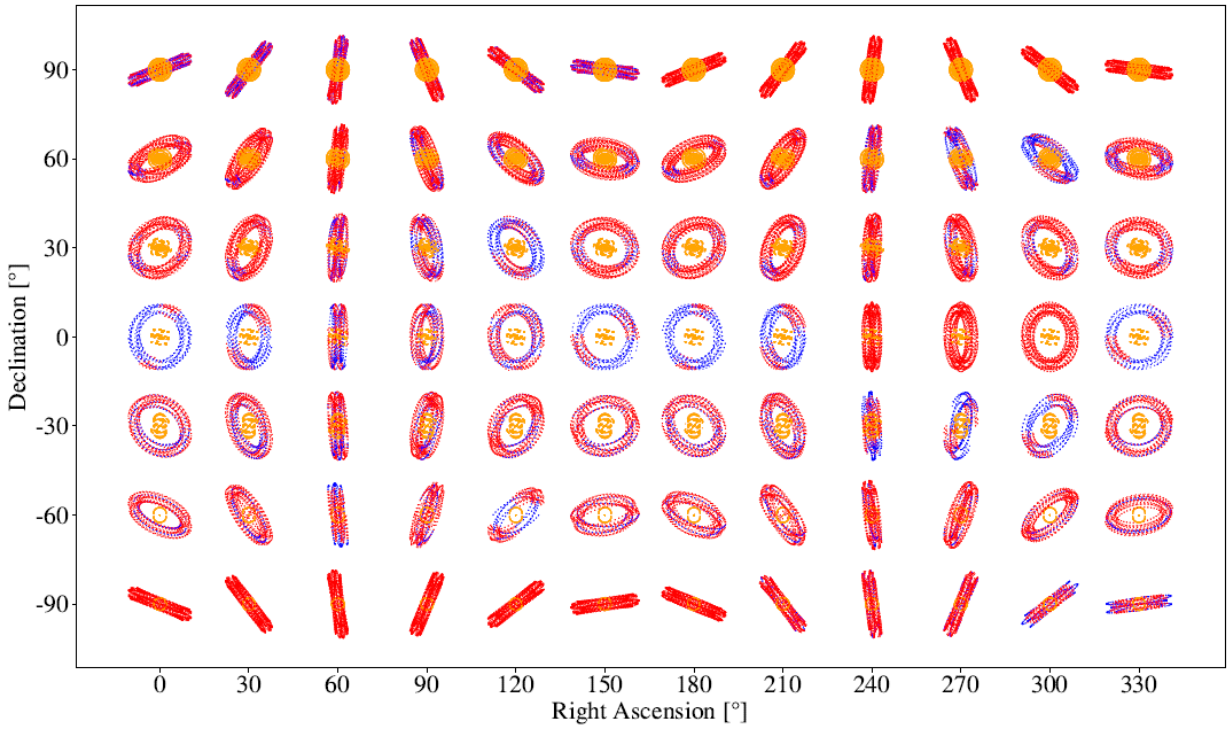

Fig. 13: All-sky (u,v) coverage achieved by BHEX of targets across the celestial sphere. The star tracker functional constraint has been included in this calculation, with the two units positioned in the 'optimal' locations determined in section 6.3. Observation of each right ascension, declination position is conducted at the time of year when the source is 180° separated from the Sun.

tions than these two SMBH targets. It has been shown how the attitude sphere can provide a clear depiction of the constraint optimisation problem. Fig. 7, 9 and 10 show the geometry of the Earth, Sun and Moon throughout observation of M87* and Sgr A*. Observation of each additional source adds another set of Earth, Sun and Moon positions to the attitude sphere that must be taken into consideration when optimising the spacecraft configuration.

Fig. 13 depicts an *all-sky (u,v)* plot for BHEX which shows the coverage achieved by the full interferometer of targets across the celestial sphere. This coverage has been calculated with inclusion of the functional constraint imposed by two star trackers. Coverage lost due to the functional constraints limiting observations is shown in red. The figure demonstrates how configurations that are 'optimal' for observing M87* and Sgr A*, are insufficient for other sources, resulting in very significant losses in *(u,v)* coverage. The figure also includes the effect of a 90° Sun exclusion and 5° Earth limb and Moon exclusion, the former resulting in total loss of coverage for some targets at high declinations.

Under the exclusion angle assumptions made in the previous sections, positioning of two star trackers and a radiator surface so that they are not blinded throughout observations is impossible given even one additional source to M87* and Sgr A*. Even the strategy described in section 6.3, flying a third star tracker, will not be sufficient as other target sources of BHEX are added to the attitude sphere. For the real-time downlink constraint, it has been shown that the impact on *(u,v)* coverage is highly dependent on the gimbal capability of the optical terminal. The effect of the real-time downlink constraint was not included in Fig. 13 as to observe different sources, unique implementations of the attitude control strategy described in section 6.1 are required. For the generation of Fig. 13, the optimal attitude control strategy to maintain the real-time downlink when observing M87* was implemented. Again, this emphasises that what is optimal for M87* and Sgr A* does not guarantee that the same observing strategies can be used by BHEX for other sources.

As such, for BHEX and future space-based VLBI missions, additional methodologies will be required to overcome the complex optimisation problem that is constraint

mitigation. The spacecraft design and mission architecture must be optimised for observation of a set of primary sources, for which the *(u,v)* coverage will be maximised. Sources located close together in the sky will be subjected to very similar constraints, as the Earth, Sun and Moon profiles on the attitude sphere will be similar. For example, 3C273 and 3C279, quasars of high scientific value for studies with BHEX, lie close to M87*. Therefore, optimising the mission for observation of carefully selected regions of sky will increase the number of sources for which the impact of constraints can be mitigated.

As described previously, another promising strategy for constraint mitigation lies in the attitude control of the spacecraft. The elements of the design for which functional constraints exist are usually based around a specific relationship with the Earth, Sun or Moon. For some constraints, this relationship is positive: the optimal location of an optical terminal is the point on the attitude sphere which provides the greatest intersection with the Earth sphere. For others it is negative: star trackers and radiator surfaces blinded by Earth, Sun (and Moon). This polarity can be taken advantage of by varying the attitude of the spacecraft throughout observations, as was described as the primary mitigation strategy in section 6.1. Proposed was a 180° rotation about the Z-axis, every half orbit period. However, if the gimbal capability of the terminal is less than the optimal ±90°, rotating the spacecraft constantly throughout an observation to keep one side near-Earth facing would increase the times at which a link with a ground station can be achieved. In contrast, as was shown in sections 6.2 and 6.3, star trackers and radiator surfaces would be provided with a mounting surface which will never be pointed towards the Earth.

The difficulty in this operation lies in the accurate pointing required of the antenna towards the target source. If rotation is conducted continuously, the spacecraft centre of mass would have to be stringently positioned to ensure the rotation axis is exactly about the antenna pointing. Furthermore, maintaining the required pointing accuracy and stability whilst rotating would be a significant challenge. A perhaps more realistic approach is to conduct discrete rotations at set intervals around the orbit, settling into an inertially-fixed attitude to perform observations. This is more feasible from an attitude control perspective but observation time would be lost during the slew and subsequent settling of the spacecraft attitude control. Variation in the polarisation of the received signals would also have to be corrected for on the ground with estimations of the spacecraft's attitude. With a control accuracy of ~arcseconds, the attitude knowledge could be expected to be an order of magnitude higher than this. This strategy may be too ambitious for missions such as BHEX with the constraints of a SMEX mission but it could be a legitimate option for future space VLBI missions.

Mission optimisation to minimise the impact of the functional constraints must also consider the required properties of the *(u,v)* coverage that is achieved for each source, depending on the science objectives. The major benefit of space VLBI is the improvement in angular resolution due to the longer baselines and prospective ability to observe at wavelengths unachievable on the ground. To achieve this, the functional constraints cannot be allowed to impact observations on the longest baselines. It is also important that baselines with key ground stations, providing the highest SNR, are maintained. Optimisation of the mission to minimise the impact of constraints is therefore not only a spacial problem, but also temporal as the spacecraft must be designed so that unavoidable constraints occur at the least impactful times.

8. Conclusion

Space-based VLBI has the potential to advance large fields of astrophysics and fundamental physics which have until now been unattainable due to the limitations of ground VLBI. BHEX will resolve the photon rings of M87* and Sgr A*, enabling precise measurements of mass and spin of these SMBHs. By achieving the finest angular resolution in the history of astronomy, BHEX will provide invaluable contributions to other areas of research such as physics of inner areas of AGN and multi-messenger astronomy through spatially-resolving generators of gravitational wave emission (SMBHBs) [36].

BHEX is the most likely space VLBI concept to be realised in the near-future. However, as described in section 2.1, numerous other mission concepts have been proposed. THEZA in particular would provide an order of magnitude improvement in angular resolution compared to ground-based systems, forming space-space baselines with no theoretical limit on observing up to terahertz frequencies. A space-based VLBI mission is unavoidable if the science objectives discussed in this paper are to be met.

VLBI is a challenging observation technique and placing one or more of the interferometer elements in space only increases the complexity of the system. VLBI places demanding requirements on the spacecraft design and some of the technological difficulties associated with such a mission have been discussed in this investigation. The primary intention of this paper is to present the functional constraints that can affect a space-based VLBI mission, impacting observations and the subsequent science return. The past space VLBI spacecraft, VSOP-HALCA and RadioAstron, provide clear examples of the impact of such constraints, and how they could have perhaps been

avoided through different design choices and technology developments.

Although analysis of the functional constraints requires assumptions to be made about the spacecraft design and mission architecture, they should be considered as early in the mission concept development as possible to identify the areas which require the greatest attention and technological development. For example, as has been shown in this paper, the preliminary choice of a real-time downlink solution to data handling for BHEX has already placed a significant constraint on the system's operation. As the BHEX concept matures, the process presented in this paper must be regularly repeated to determine whether functional constraints have been introduced/changed through design choices. The `spacevlbi` Python package has been developed to enable analysis of such constraints and it is hoped that it will be used in the design of future space-based VLBI missions.

Investigation into the functional constraints and discussion of the difficulties associated with overcoming them is not intended to question the feasibility of space-based VLBI (past missions already prove its viability). It is to ensure that the future missions are as effective as possible and that the science return of these systems is maximised. It is often the case in human history that overcoming the most difficult of challenges opens the door for the greatest accomplishments, and space-based VLBI is no different.

8.1 Future Work

In this paper, optimisation of the system parameters to minimise the impact of the functional constraints has been primarily focused on the spacecraft configuration. It has been assumed that the orbit selection is almost completely driven by the science case, whereas in reality there will be other factors that contribute to the orbit design. In future work, optimisation of the functional constraint impact will include consideration of the spacecraft's orbit. The optimisation process presented in section 5 will be expanded to include selection of the orbital elements to minimise the impact of certain constraints. This is a process that the future space VLBI missions will have to go through during detailed design and such an optimisation technique would be highly valuable during that stage of the future programmes.

The functional constraint analysis performed here has not considered more dynamic limitations on when observations can be performed. These could include constraints on how long certain pieces of equipment can be used for, either due to insufficient power provision or thermal implications. Such effects should be identified and their impact modelled as the design of BHEX and other space VLBI concepts progress.

Future work will also include space-VLBI mission concept design and optimisation with a specific focus on multi-messenger astronomy of binary SMBHs. This key area of astrophysical research was described in section 1.2. For a future space-based VLBI mission with this as its primary objective, a different configuration will be required to that of BHEX and the orbit configurations presented for THEZA in our previous work. [9]. A mission concept with a multi-messenger, binary SMBH science objective has not yet been proposed in the space VLBI literature.

Acknowledgements

The authors would like to thank Michael Johnson and the rest of the BHEX community for their ongoing efforts to realise this exciting mission. The authors are also grateful to Don Boroson, who helped define the attitude control strategy for maintaining real-time downlink.

SI is supported by Hubble Fellowship grant HST-HF2-51482.001-A awarded by the Space Telescope Science Institute, which is operated by the Association of Universities for Research in Astronomy, Inc., for NASA, under contract NAS5-26555.

References

[1] EHT, "First M87 Event Horizon Telescope Results. I. The Shadow of the Supermassive Black Hole," *Astrophysical Journal Letters*, vol. 875, p. L1, 2019. DOI: 10.3847/2041-8213/ab0ec7.

[2] EHT, "First Sagittarius A* Event Horizon Telescope Results. I. The Shadow of the Supermassive Black Hole in the Center of the Milky Way," *Astrophysical Journal Letters*, vol. 930, p. L12, 2022. DOI: 10.3847/2041-8213/ac6674.

[3] F. Roelofs, L. Blackburn, G. Lindahl, *et al.*, "The ngEHT Analysis Challenges," en, *Galaxies*, vol. 11, no. 1, p. 12, Jan. 2023, ISSN: 2075-4434. DOI: 10.3390/galaxies11010012. [Online]. Available: https://www.mdpi.com/2075-4434/11/1/12 (visited on 03/24/2023).

[4] R. S. a. T. O. Group, *RadioAstron User Handbook V2.94*, Dec. 2019. [Online]. Available: http://www.asc.rssi.ru/radioastron/documents/rauh/en/rauh.pdf (visited on 03/17/2024).

[5] Y. Murata, "VSOP/HALCA international mission operation," en, *Advances in Space Research*, vol. 26, no. 4, pp. 603–608, 2000, ISSN: 02731177. DOI: 10.1016/S0273-1177(99)01176-X. [Online]. Available: https://

linkinghub.elsevier.com/retrieve/pii/S027311779901176X (visited on 03/17/2024).

[6] L. I. Gurvits, Z. Paragi, V. Casasola, *et al.*, "THEZA: TeraHertz Exploration and Zooming-in for Astrophysics: An ESA Voyage 2050 White Paper," en, *Experimental Astronomy*, vol. 51, no. 3, pp. 559–594, Jun. 2021, ISSN: 0922-6435, 1572-9508. DOI: 10.1007/s10686-021-09714-y. [Online]. Available: https://link.springer.com/10.1007/s10686-021-09714-y (visited on 06/13/2022).

[7] *Black hole explorer*. [Online]. Available: https://www.blackholeexplorer.org/. (visited on 04/13/2024).

[8] P. L. Kurczynski, M. D. Johnson, S. S. Doeleman, *et al.*, "The Event Horizon Explorer mission concept," in *Space Telescopes and Instrumentation 2022: Optical, Infrared, and Millimeter Wave*, L. E. Coyle, M. D. Perrin, and S. Matsuura, Eds., Montréal, Canada: SPIE, Aug. 2022, p. 20, ISBN: 978-1-5106-5341-2 978-1-5106-5342-9. DOI: 10.1117/12.2630313. [Online]. Available: https://www.spiedigitallibrary.org/conference-proceedings-of-spie/12180/2630313/The-Event-Horizon-Explorer-mission-concept/10.1117/12.2630313.full (visited on 03/24/2023).

[9] B. Hudson, L. Gurvits, M. Wielgus, Z. Paragi, L. Liu, and W. Zheng, "Orbital configurations of spaceborne interferometers for studying photon rings of supermassive black holes," *Acta Astronautica*, vol. 213, pp. 681–693, 2023, ISSN: 0094-5765. DOI: 10.1016/j.actaastro.2023.09.035.

[10] M. D. Johnson, A. Lupsasca, A. Strominger, *et al.*, "Universal interferometric signatures of a black hole's photon ring," en, *Science Advances*, vol. 6, no. 12, eaaz1310, Mar. 2020, ISSN: 2375-2548. DOI: 10.1126/sciadv.aaz1310. [Online]. Available: https://www.science.org/doi/10.1126/sciadv.aaz1310 (visited on 06/02/2022).

[11] S. E. Gralla, D. E. Holz, and R. M. Wald, "Black hole shadows, photon rings, and lensing rings," en, *Physical Review D*, vol. 100, no. 2, p. 024018, Jul. 2019, ISSN: 2470-0010, 2470-0029. DOI: 10.1103/PhysRevD.100.024018. [Online]. Available: https://link.aps.org/doi/10.1103/PhysRevD.100.024018 (visited on 05/06/2023).

[12] S. E. Gralla, A. Lupsasca, and D. P. Marrone, "The shape of the black hole photon ring: A precise test of strong-field general relativity," en, *Physical Review D*, vol. 102, no. 12, p. 124004, Dec. 2020, ISSN: 2470-0010, 2470-0029. DOI: 10.1103/PhysRevD.102.124004. [Online]. Available: https://link.aps.org/doi/10.1103/PhysRevD.102.124004 (visited on 08/13/2022).

[13] A. E. Broderick, P. Tiede, D. W. Pesce, and R. Gold, "Measuring Spin from Relative Photon-ring Sizes," *The Astrophysical Journal*, vol. 927, no. 1, p. 6, Mar. 2022, ISSN: 0004-637X, 1538-4357. DOI: 10.3847/1538-4357/ac4970. [Online]. Available: https://iopscience.iop.org/article/10.3847/1538-4357/ac4970 (visited on 07/30/2023).

[14] M. Wielgus, "Photon rings of spherically symmetric black holes and robust tests of non-Kerr metrics," en, *Physical Review D*, vol. 104, no. 12, p. 124058, Dec. 2021, ISSN: 2470-0010, 2470-0029. DOI: 10.1103/PhysRevD.104.124058. [Online]. Available: https://link.aps.org/doi/10.1103/PhysRevD.104.124058 (visited on 08/30/2022).

[15] D. C. M. Palumbo, G. N. Wong, and B. S. Prather, "Discriminating Accretion States via Rotational Symmetry in Simulated Polarimetric Images of M87," *The Astrophysical Journal*, vol. 894, no. 2, p. 156, May 2020, ISSN: 0004-637X, 1538-4357. DOI: 10.3847/1538-4357/ab86ac. [Online]. Available: https://iopscience.iop.org/article/10.3847/1538-4357/ab86ac (visited on 03/22/2024).

[16] M. D. Johnson, K. Akiyama, L. Blackburn, *et al.*, "Key Science Goals for the Next-Generation Event Horizon Telescope," en, *Galaxies*, vol. 11, no. 3, p. 61, Apr. 2023, ISSN: 2075-4434. DOI: 10.3390/galaxies11030061. [Online]. Available: https://www.mdpi.com/2075-4434/11/3/61 (visited on 05/30/2023).

[17] H. Paugnat, A. Lupsasca, F. H. Vincent, and M. Wielgus, "Photon ring test of the Kerr hypothesis: Variation in the ring shape," *Astronomy & Astrophysics*, vol. 668, A11, Dec. 2022, ISSN: 0004-6361, 1432-0746. DOI: 10.1051/0004-6361/202244216. [Online]. Available: https://www.aanda.org/10.1051/0004-6361/202244216 (visited on 05/06/2023).

[18] A. P. Marscher, S. G. Jorstad, F. D. D'Arcangelo, *et al.*, "The inner jet of an active galactic nucleus as revealed by a radio-to--ray outburst," en, *Nature*, vol. 452, no. 7190, pp. 966–969, Apr. 2008, ISSN: 0028-0836, 1476-4687. DOI: 10.1038/nature06895. [Online]. Available: https://

www.nature.com/articles/nature06895 (visited on 03/22/2024).

[19] Y. Kovalev, A. Pushkarev, E. Nokhrina, *et al.*, "A transition from parabolic to conical shape as a common effect in nearby AGN jets," en, *Monthly Notices of the Royal Astronomical Society*, vol. 495, no. 4, pp. 3576–3591, Jul. 2020, ISSN: 0035-8711, 1365-2966. DOI: 10.1093/mnras/staa1121. [Online]. Available: https://academic.oup.com/mnras/article/495/4/3576/5825365 (visited on 03/22/2024).

[20] R. D. Blandford and R. L. Znajek, "Electromagnetic extraction of energy from Kerr black holes," en, *Monthly Notices of the Royal Astronomical Society*, vol. 179, no. 3, pp. 433–456, Jul. 1977, ISSN: 0035-8711, 1365-2966. DOI: 10.1093/mnras/179.3.433. [Online]. Available: https://academic.oup.com/mnras/article-lookup/doi/10.1093/mnras/179.3.433 (visited on 04/11/2024).

[21] A. Tursunov and N. Dadhich, "Fifty Years of Energy Extraction from Rotating Black Hole: Revisiting Magnetic Penrose Process," en, *Universe*, vol. 5, no. 5, p. 125, May 2019, ISSN: 2218-1997. DOI: 10.3390/universe5050125. [Online]. Available: https://www.mdpi.com/2218-1997/5/5/125 (visited on 04/11/2024).

[22] M. Colpi, "Massive Binary Black Holes in Galactic Nuclei and Their Path to Coalescence," en, *Space Science Reviews*, vol. 183, no. 1-4, pp. 189–221, Sep. 2014, ISSN: 0038-6308, 1572-9672. DOI: 10.1007/s11214-014-0067-1. [Online]. Available: http://link.springer.com/10.1007/s11214-014-0067-1 (visited on 03/22/2024).

[23] P. J. Armitage and P. Natarajan, "Accretion during the Merger of Supermassive Black Holes," en, *The Astrophysical Journal*, vol. 567, no. 1, pp. L9–L12, Mar. 2002, ISSN: 0004-637X, 1538-4357. DOI: 10.1086/339770. [Online]. Available: https://iopscience.iop.org/article/10.1086/339770 (visited on 03/22/2024).

[24] M. Milosavljević, "The Final Parsec Problem," en, in *AIP Conference Proceedings*, ISSN: 0094243X, vol. 686, College Park, Maryland (USA): AIP, 2003, pp. 201–210. DOI: 10.1063/1.1629432. [Online]. Available: https://pubs.aip.org/aip/acp/article/686/1/201-210/583670 (visited on 03/22/2024).

[25] A. Mangiagli, C. Caprini, M. Volonteri, *et al.*, "Massive black hole binaries in lisa: Multimessenger prospects and electromagnetic counterparts," *Phys. Rev. D*, vol. 106, p. 103 017, 10 Nov. 2022. DOI: 10.1103/PhysRevD.106.103017. [Online]. Available: https://link.aps.org/doi/10.1103/PhysRevD.106.103017.

[26] H. Hirabayashi, H. Hirosawa, H. Kobayashi, *et al.*, "Overview and Initial Results of the Very Long Baseline Interferometry Space Observatory Programme," *Science*, vol. 281, p. 1825, Sep. 1998. DOI: 10.1126/science.281.5384.1825.

[27] H. Hirabayashi, H. Hirosawa, H. Kobayashi, *et al.*, "The VLBI Space Observatory Programme and the Radio-Astronomical Satellite HALCA," *Publications of the Astronomical Society of Japan*, vol. 52, pp. 955–L965, Dec. 2000, ADS Bibcode: 2000PASJ...52..955H, ISSN: 0004-6264. DOI: 10.1093/pasj/52.6.955. [Online]. Available: https://ui.adsabs.harvard.edu/abs/2000PASJ...52..955H (visited on 03/17/2024).

[28] N. S. Kardashev, V. V. Khartov, V. V. Abramov, *et al.*, ""RadioAstron"-A telescope with a size of 300 000 km: Main parameters and first observational results," en, *Astronomy Reports*, vol. 57, no. 3, pp. 153–194, Mar. 2013, ISSN: 1063-7729, 1562-6881. DOI: 10.1134/S1063772913030025. [Online]. Available: http://link.springer.com/10.1134/S1063772913030025 (visited on 11/19/2022).

[29] A. Fuentes, J. L. Gómez, J. M. Martí, *et al.*, "Filamentary structures as the origin of blazar jet radio variability," *Nature Astronomy*, vol. 7, pp. 1359–1367, Nov. 2023. DOI: 10.1038/s41550-023-02105-7. arXiv: 2311.01861 [astro-ph.HE].

[30] L. I. Gurvits, "Space VLBI: From first ideas to operational missions," en, *Advances in Space Research*, vol. 65, no. 2, pp. 868–876, Jan. 2020, ISSN: 02731177. DOI: 10.1016/j.asr.2019.05.042. [Online]. Available: https://linkinghub.elsevier.com/retrieve/pii/S0273117719303886 (visited on 07/30/2023).

[31] F. Roelofs, H. Falcke, C. Brinkerink, *et al.*, "Simulations of imaging the event horizon of Sagittarius A* from space," *Astronomy & Astrophysics*, vol. 625, A124, May 2019, ISSN: 0004-6361, 1432-0746. DOI: 10.1051/0004-6361/201732423. [Online]. Available: https://www.aanda.org/10.1051/0004-6361/201732423 (visited on 11/19/2022).

[32] V. Kudriashov, M. Martin-Neira, F. Roelofs, *et al.*, "An Event Horizon Imager (EHI) Mission Concept Utilizing Medium Earth Orbit Sub-mm Interferometry," *Chinese Journal of Space Science*, vol. 41, no. 2, p. 211, 2021, ISSN: 0254-6124, 0254-6124. DOI: 10.11728/cjss2021.02.211. [Online]. Available: https://www.sciengine.com/doi/10.11728/cjss2021.02.211 (visited on 03/17/2024).

[33] A. Shlentsova, F. Roelofs, S. Issaoun, J. Davelaar, and H. Falcke, "Imaging the event horizon of M87* from space on different timescales," 2024, Publisher: [object Object] Version Number: 1. DOI: 10.48550/ARXIV.2403.03327. [Online]. Available: https://arxiv.org/abs/2403.03327 (visited on 03/17/2024).

[34] S. Trippe, T. Jung, J.-W. Lee, *et al.*, "Capella: A Space-only High-frequency Radio VLBI Network Formed by a Constellation of Small Satellites," *arXiv e-prints*, arXiv:2304.06482, arXiv:2304.06482, Apr. 2023. DOI: 10.48550/arXiv.2304.06482. arXiv: 2304.06482 [astro-ph.IM].

[35] V. L. Fish, M. Shea, and K. Akiyama, "Imaging black holes and jets with a VLBI array including multiple space-based telescopes," *Advances in Space Research*, vol. 65, no. 2, pp. 821–830, Jan. 2020. DOI: 10.1016/j.asr.2019.03.029.

[36] M. D. Johnson, K. Akiyama, R. Baturin, *et al.*, "The Black Hole Explorer: Motivation and Vision," *arXiv e-prints*, arXiv:2406.12917, arXiv:2406.12917, Jun. 2024. DOI: 10.48550/arXiv.2406.12917. arXiv: 2406.12917 [astro-ph.IM].

[37] J. P. Wang, B. Bilyeu, D. Boroson, *et al.*, "High-rate 256+ Gbit/s laser communications for enhanced high-resolution imaging using space-based very long baseline interferometry (VLBI)," in *Society of Photo-Optical Instrumentation Engineers (SPIE) Conference Series*, H. Hemmati and B. S. Robinson, Eds., ser. Society of Photo-Optical Instrumentation Engineers (SPIE) Conference Series, vol. 12413, Mar. 2023, 1241308, p. 1 241 308. DOI: 10.1117/12.2651471.

[38] D. P. Marrone, J. Houston, K. Akiyama, *et al.*, *The Black Hole Explorer: Instrument System Overview*, Version Number: 1, 2024. DOI: 10.48550/ARXIV.2406.10143. [Online]. Available: https://arxiv.org/abs/2406.10143 (visited on 08/15/2024).

[39] L. I. Gurvits, Z. Paragi, R. I. Amils, *et al.*, "The science case and challenges of space-borne sub-millimeter interferometry," *Acta Astronautica*, vol. 196, pp. 314–333, 2022, ISSN: 0094-5765. DOI: https://doi.org/10.1016/j.actaastro.2022.04.020. [Online]. Available: https://www.sciencedirect.com/science/article/pii/S0094576522001692.

[40] A. A. Chael, M. D. Johnson, K. L. Bouman, L. L. Blackburn, K. Akiyama, and R. Narayan, "Interferometric Imaging Directly with Closure Phases and Closure Amplitudes," *The Astrophysical Journal*, vol. 857, no. 1, p. 23, Apr. 2018, ISSN: 0004-637X, 1538-4357. DOI: 10.3847/1538-4357/aab6a8. [Online]. Available: https://iopscience.iop.org/article/10.3847/1538-4357/aab6a8 (visited on 08/15/2024).

[41] D. F. D. Silva, I. Muraoka, F. L. D. Sousa, and E. C. Garcia, "Multiobjective and Multicase Optimization of a Spacecraft Radiator," *Journal of Aerospace Technology and Management*, vol. 11, Jan. 2019, ISSN: 2175-9146. DOI: 10.5028/jatm.v11.1000. [Online]. Available: http://www.jatm.com.br/ojs/index.php/jatm/article/view/1000 (visited on 03/27/2024).

[42] F. J. T. Salazar and F. G. M. de Carvalho, "Star tracker orientation optimization using non-dominated sorting genetic algorithm (nsga)," in *2014 IEEE Aerospace Conference*, 2014, pp. 1–8. DOI: 10.1109/AERO.2014.6836461.

[43] R. S. Park, W. M. Folkner, J. G. Williams, and D. H. Boggs, "The JPL Planetary and Lunar Ephemerides DE440 and DE441," *The Astronomical Journal*, vol. 161, no. 3, p. 105, Mar. 2021, ISSN: 0004-6256, 1538-3881. DOI: 10.3847/1538-3881/abd414. [Online]. Available: https://iopscience.iop.org/article/10.3847/1538-3881/abd414 (visited on 03/27/2024).

[44] C. M. Schieler, K. M. Riesing, B. C. Bilyeu, *et al.*, "On-orbit demonstration of 200-Gbps laser communication downlink from the TBIRD CubeSat," in *Free-Space Laser Communications XXXV*, H. Hemmati and B. S. Robinson, Eds., San Francisco, United States: SPIE, Mar. 2023, p. 1, ISBN: 978-1-5106-5931-5 978-1-5106-5932-2. DOI: 10.1117/12.2651297. [Online]. Available: https://www.spiedigitallibrary.org/conference-proceedings-of-spie/12413/2651297/On-orbit-demonstration-of-200-Gbps-laser-communication-downlink-from/10.1117/12.2651297.full (visited on 03/24/2024).

[45] J. Rigby, G. Sonneborn, J. Pollizzi, T. Brown, and J. Isaacs, *Science Operations with the James Webb Space Telescope*, 2012. [Online]. Available: https://ntrs.nasa.gov/api/citations/20120014229/downloads/20120014229.pdf.

[46] H. Rana, K. Akiyama, E. Canavan, *et al.*, *The Black Hole Explorer Cryocooling Instrument*, Version Number: 1, 2024. DOI: 10.48550/ARXIV.2406.09975. [Online]. Available: https://arxiv.org/abs/2406.09975 (visited on 08/16/2024).

[47] F. L. Markley and J. L. Crassidis, *Fundamentals of Spacecraft Attitude Determination and Controls* (Space Technology Library), eng. Microcosm Press and Springer, 2014, ISBN: 978-1-4939-0802-8.

[48] D. Smith, *Astrophysics and heliophysics explorers program*. [Online]. Available: https://explorers.gsfc.nasa.gov/missions.html#:~:text=Small%20Explorers%20(SMEX),million%20total%20cost%20to%20NASA. (visited on 04/13/2024).